IL NUOVO CIMENTO VOL. 17 C, N. 1 Gennaio-Febbraio 1994

A Technical Description of the TSS-1 ROPE Investigation.

N. H. STONE ([1]), K. H. WRIGHT jr. ([2]), J. D. WINNINGHAM ([3])
J. BIARD ([3]) and C. GURGIOLO ([3])

([1]) *ES53, NASA/Marshall Space Flight Center - Huntsville, AL 35812, USA*
([2]) *CSPAR, University of Alabama in Huntsville - AL 35899, USA*
([3]) *Div. 15, Southwest Research Institute - San Antonio, TX 78228, USA*

(ricevuto il 22 Aprile 1993; approvato il 30 Giugno 1993)

Summary. – The Research on Orbital Plasma Electrodynamics (ROPE) investigation was designed to study the complex of phenomena and processes expected to exist around the highly biased satellite of the TSS-1 system. Specifically, ROPE was to study the characteristics of the high-voltage sheath and study ionization processes in the vicinty of the satellite. To accomplish this, two banks of sensors were mounted on the satellite. One was flush-mounted on the satellite's surface and the other was located at the end of the satellite's fixed boom. Of particular note is the ability to drive the boom probes' surface potential to the local floating potential. In conjunction with satellite spin, the surface-mounted sensors could map the distribution of electron flux to the satellite's surface while the boom-mounted sensors could measure the ion and electron fluxes in and out of the satellite's plasma sheath.

PACS 94.80 – Atmospheric instrumentation.
PACS 52.40 – Plasma interactions.
PACS 52.70 – Plasma diagnostic techniques and instrumentation.

1. – Introduction.

1·1. *Experiment objectives.* – One objective of the ROPE investigation was to study the complex of phenomena and processes expected to exist around the satellite as it travels at mesothermal speeds, becomes highly biased and extracts electrons from the ionospheric plasma. For example, the satellite was expected to attain potentials of several kilovolts and the measurements obtained from the ROPE instruments would provide a unique opportunity to investigate the resulting high-voltage plasma sheath. In addition, the way in which current would flow through the sheath to the satellite, how this current would be distributed and affected by the geomagnetic field, and the magnitude of such a current as

a function of the ambient ionospheric parameters and the magnitude of the voltage developed across the tether, were also questions of interest. Finally, the ROPE instrumentation was specifically developed to allow investigation of ionization processes and the possible trapping of suprathermal electrons in the vicinity of the satellite.

These objectives require that the ROPE instruments determine the energy and spatial distributions of charged particle fluxes to the surface of the satellite and the charged-particle energy distributions in its near vicinity. The ROPE instruments were also required to measure the satellite's electric potential and the space potential within the satellite's plasma sheath. The relationship of these measurements to the other TSS-1 investigations is discussed in Dobrowolny and Stone [1].

1·2. *The predicted* TSS-1 *environment.* – Because the electrodynamic interaction of the TSS with the ionosphere was expected to produce highly non-equilibrium conditions, including accelerated particles and perturbed electric and magnetic fields, several theoretical studies were conducted to provide some insight into what this environment might be like and how it could affect TSS electrodynamic operations and the diagnostic measurements. In particular, these models all predict that 1) the energy distributions of ambient ionospheric electrons would become highly spiked (compressed into a small energy band) as they were accelerated into the satellite, 2) that the electrons could be magnetically screened from the satellite's surface under certain conditions, and 3) that their angle of arrival at the surface could be far different from the surface normal. At high tether voltages, an additional complexity would probably occur that is usually not considered in theoretical treatments; *i.e.* neutral particles, either from the ambient ionosphere (1000 times greater density than the ionospheric charged particles) or from satellite off-gassing, could be ionized by the energetic electrons accelerated toward the satellite as a result of the electric field in the sheath.

2. – ROPE **experiment design.**

2·1. *Overview of* ROPE *electronics and satellite interfaces.* – The ROPE experiment consists of five electronics boxes that control six sensors. The interrelationship among the various ROPE components is shown in the functional block diagram of fig. 1. The Central Electronics Package (CEP) controls the overall experiment and provides the power, data, and command interfaces to the satellite. The two High-Voltage Units (HVU1 and HVU2) provide sweep and bias voltages to the five Soft-Particle Energy Spectrometers (SPES). The Floating Supply (FS) provides a bias voltage for the boom-mounted sensors. In essence, it provides a reference voltage between the satellite and the units identified on the right side of fig. 1. The FS has an optically isolated data interface to the CEP. The Differential Ion Fux Probe-Electronics (DIFP-E) provide the operational control for the Differential Ion Flux Probe-Sensor (DIFP-S). ROPE is divided into two independent sensor banks (as is discussed in the next section) and, therefore, two power lines (1.5 A and 3 A) are needed. The 1.5 A line powers the CEP, HVU1, and SPES-3, -4, and -5; while the 3 A line powers the FS, HVU2, SPES-1 and -2, DIFP-E, and DIFP-S.

The CEP provides a telemetry interface to the satellite On-Board Data Handler

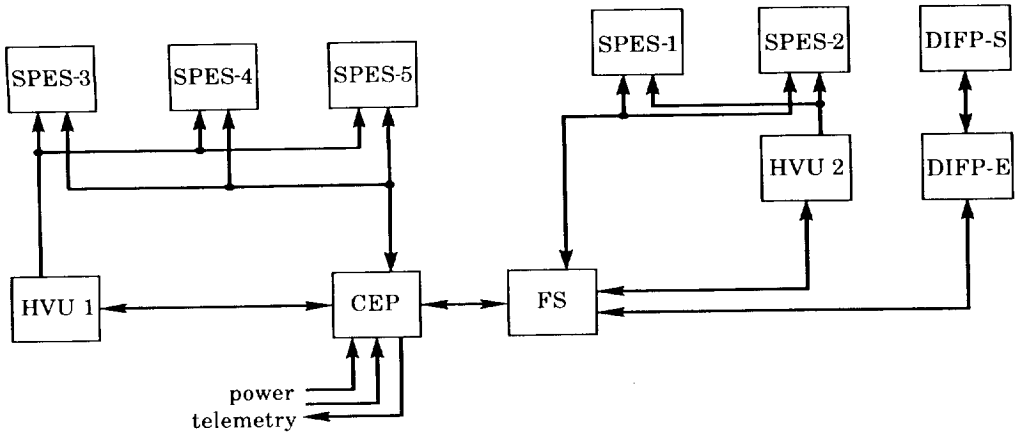

Fig. 1. – Functional block diagram of the ROPE instrumentation showing the interrelationship among the various components.

(OBDH). The CEP can receive 16-bit command words from the ground through the OBDH and store them in a command buffer that is 512 bytes long. Once every four satellite major frames (65.536 s), the CEP interrogates and processes the buffered commands. (Note that the ROPE experiment can only change its operational state once every 65.536 s.) The CEP interprets and executes commands for the HVU1 and the FS while passing those commands intended for the HVU2 and the DIFP-E to the FS for interpretation and execution. The CEP data output consists of 29 8-bit words every satellite minor frame (64 ms).

2·2. *Type sensors and mounting locations.* – The unique environment of the TSS demands that the instrumentation require no *a priori* assumptions such as the existence of thermodynamic equilibrium or as to the form of particle distributions present. Therefore, simple bare electrode sensors, such as the Langmuir probe, do not provide reliable measurements in this application. With this in mind, two types of sensors were selected for the ROPE investigation. The DIFP uses internal electrostatic fields to determine the flow direction and energy distribution of ions, while the SPES uses a form of electrostatic energy analysis to determine the energy distributions of both ions and electrons. Moreover, because each SPES sensor measures both the ion and electron energy distributions simultaneously, it is also possible to determine the local space potential.

Both of the types of sensors have an extensive flight heritage, as required by the TSS program. However, the application on this mission was unique and the way in which the sensors were used was new. To maximize the probability of success in this new application, extensive plasma tests were conducted in the space plasma simulation facilities at the NASA/Marshall Space Flight Center. The details of the DIFP and SPES instrument designs are presented in later sections.

The ROPE sensors were divided into two banks: surface mounted and boom mounted. The three surface-mounted SPES sensors were placed along a satellite longitude as illustrated in fig. 2*a*). The distribution of SPES sensors along a satellite longitude coupled with satellite spin allows the charged-particle flux to the upper hemisphere of the satellite's surface to be mapped.

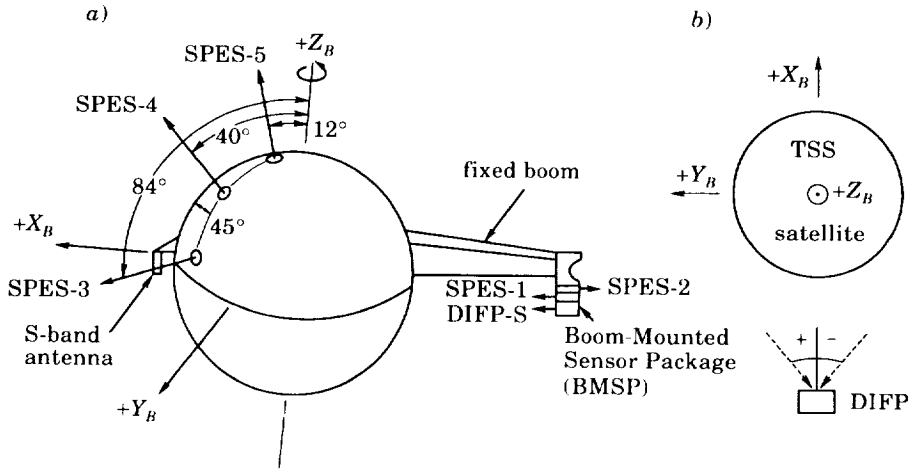

Fig. 2. – *a*) SPES and DIFP sensor-mounting arrangements on the TSS satellite. Nominal mounting angles for SPES-3, -4, -5 are shown. The satellite body coordinate system is indicated by the X_B, Y_B, Z_B axes. *b*) Geometric reference system for DIFP ion stream angle measurements. The angle subtended by satellite at DIFP location is $\pm$ 25.5°.

A second bank of sensors was placed on the satellite's fixed boom approximately one body radius away from the satellite's surface. The Boom-Mounted Sensor Package (BMSP) consisted of two SPES sensors and one DIFP sensor. The BMSP SPES-1 sensor was pointed directly at the satellite to measure electrons and ions flowing out of the sheath while the SPES-2 sensor was pointed radially away from the satellite to detect incoming electrons. The DIFP sensor was also pointed directly at the satellite. With its ability to determine ion flow direction and energy, the DIFP can distinguish between ions that are born within the sheath by ionization, ambient plasma ions flowing around the satellite and into the wake, and ambient ions reflected by the biased satellite. The reference system for DIFP measurements of the ion flow direction is indicated in fig. 2*b*).

2·2.1. DIFP instrument description. The DIFP is capable of deconvolving several coincident ion streams (differing in flow direction and/or energy) and independently determining the flow direction, current density, and energy distribution of each stream. The DIFP was developed for laboratory investigations of the interaction between a body and a collisionless, flowing plasma [2]. Later, the DIFP was developed for flight on the STS-3 and Spacelab-2 shuttle missions [3] and for the CENTAUR sounding rocket campaigns.

The DIFP sensor head consists of an Electrostatic Deflection and Collimation System (EDCS) mounted in front of a planar, gridded retarding potential analyzer (RPA). In principal, the flight model of the DIFP operates like the laboratory model as described in Stone [2]. A stream of ions arriving at the entrance slit with some angle of attack θ, which lies in a plane perpendicular to the collimation slits (the «analysis plane»), and with some energy, E, will be deflected through the exit slit by applying a specific potential, ϕ_d, of opposite polarity to the deflection plates. At any given deflection potential, the instantaneous field of view in the analysis

plane is limited by the EDCS geometry to approximately $\Delta\theta$ (there is a second-order increase with ϕ_d). Therefore, by sweeping ϕ_d, the DIFP can differentially scan over the angular range of $\pm\ \Omega$ (see fig. 3). If the ion energy is increased, a higher potential must be applied to the plates to deflect the ions the same amount for any value of θ. Therefore, the EDCS can be viewed as an energy-angle filter which operates such that at any given deflection potential, ϕ_d, the energy and angle of the admissible ion must satisfy a known relation, $f(\theta, E) = \phi_d$, where the function f is a characteristic of the EDCS design. After passing through the EDCS, the ions enter the RPA section at an angle α which is much smaller than θ. Ion energy, due to the velocity component normal to the grids, is proportional to the potential at which the ions are retarded and can, therefore, be determined by sweeping the retarding potential, ϕ_r. The measured values of ϕ_d and ϕ_r then provide two known variables that can be used to determine the two unknown characteristics of the ions, θ and E.

A schematic of the flight model DIFP sensor head is shown in fig. 3. An entrance plate and two collimation plates make up the EDCS. The entrance plate contains ten parallel slits, each flanked by a set of deflection plates on the lower side. Each slit is 2.50 cm by 0.16 cm, providing an effective aperture area of 4.0 cm^2. The inter-slit spacing is 0.20 cm. The deflection plates are 0.11 cm by 2.54 cm and tilted 45 degrees with respect to the aperture plane. Two sets of collimation plates exist between the entrance and exit plane to prevent cross talk (*i.e.* to isolate ions entering each column of slits from all other columns). Details on construction of the entrance slit-deflection plate system can be found in Stone *et al.* [3].

Trajectory analysis and subsequent calibration measurements performed in the

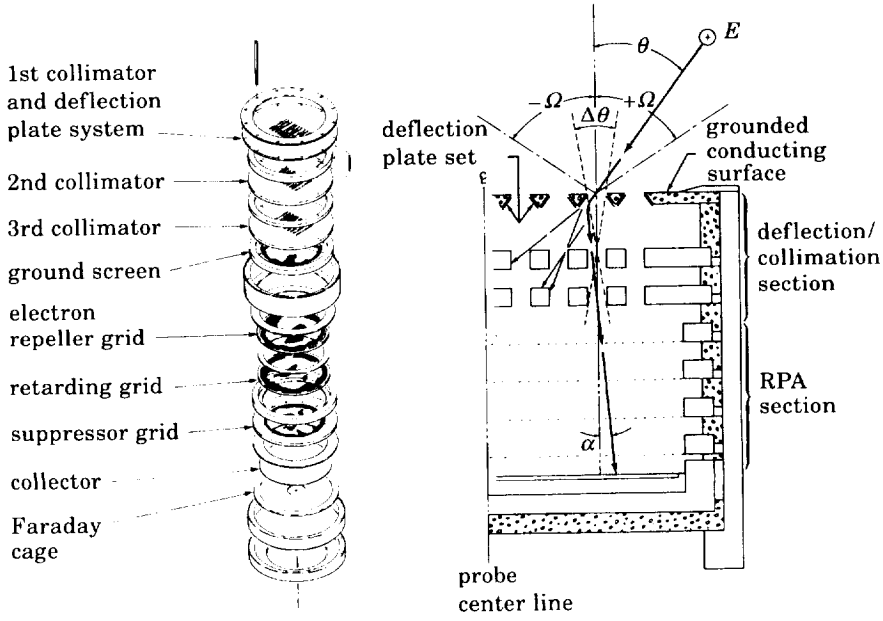

Fig. 3. – Schematic of DIFP (after Stone *et al.* [3]).

space plasma simulation facility at NASA/MSFC have established that, for the multislit design, $\Delta\theta = 5$ degrees, $\alpha < 5$ degrees, and $\Omega = 60$ degrees. The instrument characteristic function is

$$\phi_d/E = A_1 \sin(B_1\theta), \tag{1}$$

where $A_1 = 1.34 \pm 0.14$ and $B_1 = 1.44 \pm 0.10$. The range of A_1 and B_1 is due to the spread of points in the calibration data at the higher angles. In addition these values were determined for out-of-analysis plane angles approximately zero. How A_1 and B_1 vary with out-of-plane angle (θ_0) is currently under study. The variation of the collected current as a function of angle of attack (*i.e.* the anguar sensitivity) is given by

$$I(\theta) = I_0 \exp[A_2\theta^2 + B_2\theta^4], \tag{2}$$

where I_0 = collected current for $\theta = \theta_0 = \phi_d = \phi_r = 0$, $A_2 = -(1.35 \mp 0.35) \cdot 10^{-3}$, and $B_2 = (1.54 \mp 1.5) \cdot 10^{-7}$. The current collected at $\theta = \theta_0 = 0$ can also be written as (for relatively high Mach number flows)

$$I_0 = \gamma\beta e n_i V_i A, \tag{3}$$

where γ ($= 0.35$) is the stripping factor of the collimator stack compared to a conventional RPA design, β ($= 0.9^4 = 0.6561$) is the grid transmission factor, e is the ionic charge, n_i is the ion density, V_i is the ion drift velocity, and A ($= 4.0$ cm^2) is the total aperture area. There is also an angular sensitivity and energy variation in the out-of-plane angle, θ_0. The angular sensitivity is given by

$$I(\theta_0) = I_0 \exp[A_3\theta_0^2 + B_3\theta_0^4], \tag{4}$$

where I_0 = collected current for $\theta_0 = \theta = \phi_d = \phi_r = 0$, $A_3 = -(7.25 \mp 1.55) \cdot 10^{-4}$, and $B_3 = -(5.52 \pm 3.74) \cdot 10^{-8}$. The energy, E, varies approximately as $\cos^2\theta_0$.

The TSS-1 DIFP electronics have been upgraded considerably since the Spacelab 2 version (described by Stone *et al.* [3]). The new features include microprocessor control, an automatic ranging electrometer with a dynamic range of 10^{-9} to 10^{-6} A, four voltage sweep ranges, four operational modes, and an autoranging RPA sweep. The four operation modes are: 1) standard peak detect analysis; 2) deflection only; 3) retard only; and 4) electrometer. Mode 1 is interactive between the deflection and retard sweeps—ϕ_d is swept until a current peak is detected. The ϕ_d is held constant while ϕ_r completes a full sweep. The ϕ_d sweep then continues from the voltage at which it is held constant and the sequence repeats up to three times or until the end of the ϕ_d ramp occurs. The ϕ_d ramp will detect any number of ion streams present, however, an energy analysis will only be made of the first three. Modes 2 and 3 are subsets of the basic mode in that only one voltage sweep is active. In the electrometer mode no voltage sweep is active and in essence the DIFP is a narrow-aperture Faraday cup that can give information on temporal variations of ion flux density in the plasma. The voltage sweep ranges are 12.5, 25, 50, and 100 V. The deflection sweeps are bipolar, while the retarding potential sweeps from zero to positive values. In the autorange mode

for the retard sweep, the microprocessor chooses a range such that the collected current is cut off somewhere between 25% and 75% of the full range. A complete ϕ_r sweep requires 100 ms, while the ϕ_d sweep requires 200 ms. Instrument cycle time depends on the number of streams present; *i.e.* for two streams the cycle time would be 200 ms deflection $+ 2 \times 100$ ms retard $= 400$ ms.

The voltage sweeps run asynchronous to the telemetry. When any voltage sweep mode is executed, 256 pairs of voltage, current measurements are fed to the microprocessor. Only a fraction of these measurement pairs can be passed through the telemetry. A special routine is used to select the measurements containing the most «information» about a complete sweep. Points are randomly selected and tested to see if they fall into the cut-off region of the expected response curve, and are selected or rejected based on criticality or randomness. This produces deflection sweep data that is randomly sampled but «weighted» so that 75% of the data points occur on the current peak and above the FWHM level. Similarly, the retard sweep is randomly sampled but «weighted» so that 75% of the data points lie on the current drop-off.

The DIFP telemetry data block is 16 minor frames long and occupies 14 words per minor frame in the single data mode. Each word consists of 8 bits. An additional telemetry packing mode, called «double data», also exists. In this mode 32 minor frames with 14 words per minor frame are used to pass the DIFP data from a single instrument operational cycle. Greater «curve» resolution is obtained in this mode but it provides only half the temporal resolution.

2'2.2. SPES instrument description. The SPES is composed of a divergent-plate electrostatic analyzer similar to those flown in the ISIS [4], Dynamics Explorer [5], and UARS [6] programs. SPES can perform a differential spectral measurement over the energy range 0.5 eV to 27.5 keV. A diagram of a single SPES sensor unit is shown in fig. 4. It shows the positions of the deflection plates relative to the entrance aperture, collimator, the light trap, repeller screens, and the particle-sensing elements (Channel Electron Multipliers or CEMs). Incident particle energies are selected by stepping the voltage on oppositely biased deflection plates. Electrons and positive ions passing through the collimator are deflected in the region between the plates: electrons toward the CEM on the right, ions toward the CEM on the left. The particles produce pulses from the CEMs (Galileo channeltrons) that are amplified by A101 amplifier/discriminators and sent to the CEP or FS for accumulating and multiplexing into the ROPE data stream.

The analyzer constant k, sometimes called the deflection sensitivity, is the constant of proportionality relating the incident-particle energy, E, and the potential difference, ΔV, between the deflection plates. This constant and the energy resolution $\Delta E/E$ are dependent on the electrical and mechanical characteristics and condition of the surfaces of the collimation, deflection, and sensing systems shown in fig. 4. These factors, determined by a combination of laboratory calibration and detector numerical simulation, are shown in table I. To reduce UV reflection and secondary emission, the surfaces of the deflection plates, the light trap exterior, and the repeller screens were coated with gold black. This coating was selected because of its low yield of UV-generated secondary electrons.

The energy range 0.5 eV to 27.5 keV is divided into 127 equally spaced logarithmic levels. An energy spectrum is measured by stepping the voltage on the

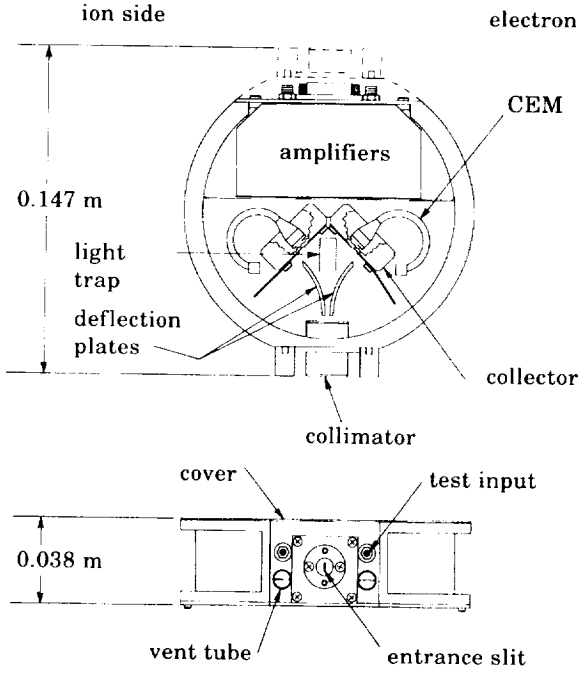

Fig. 4. – Schematic of SPES (after Winningham *et al.* [5]).

TABLE I. – SPES *characteristics. For each* SPES, *the deflection sensitivity is* 13 eV/V *and the energy resolution,* $\Delta E/E$, *is* 0.15. *The geometric factor includes screen transparencies within the sensor.*

SPES No.	Satellite orientation (θ, ϕ) [(a)]	Geometric factor (cm^2-str)	
		electron	ion
1	0°, 0°	1.24×10^{-8}	1.24×10^{-7}
2	0°, 180°	1.24×10^{-8}	1.24×10^{-7}
3	7.1°, 44.9°	1.26×10^{-7}	1.24×10^{-7}
4	50.2°, 45.3°	1.375×10^{-11}	—
5	77.9°, 44.8°	1.375×10^{-11}	—

(a) θ = elevation angle from satellite equatorial plane. Positive angles in the $+Z_B$ hemisphere. ϕ = azimuth angle from $+X_B$ axis. Positive angle counterclockwise toward $+Y_B$.

deflection plates through a subset of 31 steps between two selectable endpoints. The voltage steps occur at the minor frame rate so that 31 minor frames are required for a complete SPES spectrum. On each step, counts are accumulated for 57.3 ms. Simultaneous electron and ion spectral measurements are repeated every 2.048 s. Three energy ranges are preprogrammed: low (0.7–133 eV); medium (0.7 eV–1.8 keV); and high (4.2 eV–10.1 keV).

SPES operates in a single «spectral measurement» mode. When the instrument is «ON», electron and ion measurements are made continuously. It is possible, by ground command, to change the voltages applied to the repeller screens in order to reduce the flux on the CEMs. The normal value applied to the screens is 1 volt (-1 V on the electron screen and $+1$ V on the ion screen). These voltages can be changed to ± 5 V, respectively. For the ambient ionosphere, the screen serves effectively as a cut-off at the low end of the energy spectrum. Because of the sharp increase in number flux with decreasing energy of the spectrum in the few-eV region, a change from lower to higher voltage will significantly reduce the flux striking the CEMs.

As discussed in subsect. 1·2, the energy distributions of ambient ionospheric electrons could become concentrated into a small energy band as they are accelerated into the highly biased satellite. To avoid «burning out» the channeltrons, very small apertures are used on each SPES to limit the number of particles striking a channeltron surface. These small aperatures prevented a laboratory calibration of the SPES. Instead, numerical simulation of the SPES detector was performed in order to determine the energy and angle calibration.

Data obtained from the numerical simulations yielded values of energy resolution ($\Delta E/E$) and deflection constant (k) for specific angular orientations and for integration over all angles. A field of view of 2.5 degrees × 10 degrees at the full-width-half-maximum value was used in the calculations. Likewise, the angular responses along both axes of the rectangular apertures were determined at single energies.

Completing the numerical calibration required a determination of the detector throughput function, which includes the CEM efficiency as a function of energy. The counts accumulated by a SPES detector in time $\mathrm{d}t$ when measuring a charged particle flux $j(E)$ is

$$c = j(E)\, G(E)\, \eta(E)\, \mathrm{d}E\, \mathrm{d}t, \tag{5}$$

where $G(E)$ is the energy-dependent geometric factor of the analyzer, $\eta(E)$ is the CEM efficiency, and $\mathrm{d}E$ is the energy band pass at FWHM. An alternate form of eq. (5) is

$$c = j(E)\, GF(E)\, \mathrm{d}E\, \mathrm{d}t, \tag{6}$$

where G is the (constant) physical geometric factor of the analyzer and $F(E)$ is the energy-dependent part of the throughput function. Although the largest influence on the shape of $F(E)$ is the dependence of secondary electron production on energy, $F(E)$ will also contain any variation with energy of the analyzer response not accounted for by the physical geometric factor. To a very high degree of accuracy, all count-*vs.*-energy curves can be described with a single function, $F(E)$, by multiplying each curve by a single factor. This factor was used to compute each physical geometric factor G, thus providing accurate relative geometric-factor measurements for all SPES analyzers. Completing the calculation of the throughput function required using computations of CEM efficiency made by Bordoni [7]. The electron transfer function for electrons is a function of energy, while that for ions is a constant value of 0.65. Summary characteristics for each SPES detector are given in table I.

2·3. *Boom-mounted sensor bias control.* – While the satellite can be driven to high positive potentials by the tether voltage, it is necessary for the BMSP instruments to remain near the local-plasma potential. The BMSP is, therefore, electrically isolated from the satellite through the Floating Supply (FS) — which effectively places a 700 kΩ resistance between the two objects. The FS biasing of the BMSP relative to the satellite can be operated in two modes. In the manual mode, the FS output can be commanded to specific DC levels over a dynamic range of 0 to − 500 V, with a minimum step size of 0.122 V. By executing a sequence of such commands, the BMSP could be forced to step through a range of potentials and, thereby, serve as a type of Langmuir probe This should prove useful, for example, during periods when the satellite is forced to float by the Shuttle-based tether current control and monitoring system. In the interactive mode, as long as the satellite is less than + 500 V, the FS output is automatically adjusted to minimize the current collected by the BMSP. By driving the current down near zero, the BMSP potential will be near the local-plasma floating potential—which is normally within a few tenths of a volt of the space potential (plasma ground).

There are two parts to the interactive control algorithm: an initial seek routine, in which the FS bias voltage is continually varied until the BMSP current is «in the neighborhood» of the zero net current point, and a track routine, in which the bias voltage is adjusted to keep the BMSP potential within a window about the zero net current point. Both the seek and track routines operate on the FS bias level once each satellite minor frame, or once every 64 ms. In both routines, the control variable is the BMSP current.

When the command that initiates active bias voltage control is implemented, the FS voltage level is set to 0 V. The seek routine, during the first minor frame, checks the polarity of the BMSP current monitor. (The polarity of the BMSP current monitor is in the «Langmuir probe» convention where a positive value indicates electron collection on the BMSP surface. Conversely, a negative value indicates ion collection.) If the current monitor indicates electron collection, meaning that the BMSP is positive with respect to the local plasma, the routine increments the FS bias voltage by − 15.629 V. The new FS voltage level is implemented at the beginning of the next minor frame. This process is repeated up to 31 times. If any check of the BMSP current monitor, including the first, indicates that the current is within a window of − 1.1 μA to + 2.82 μA about zero, the seek routine terminates. The resolution of the current monitor is 0.98 μA. If the seek routine completes 31 increments of the FS voltage without reversing the BMSP current, the FS bias voltage will be held constant at − 484.49 V.

Once the seek routine has terminated, the track routine begins in the next minor frame. In this case, the control algorithm is more complicated. If the BMSP current is within the «zero» window mentioned above, the track routine takes no action. If the current level is outside the window, the track routine controls the FS voltage to drive the BMSP current level back within the zero window. In the first minor frame in which the BMSP current is out of limits, the voltage is changed by the minimum step, or 0.122 V. The polarity of the BMSP current determines the direction of the voltage step. If the BMSP current is not driven within the zero window by the next minor frame, the FS voltage is changed by two minimum steps, or 2.244 V. This process is repeated with the FS voltage step size doubling each minor frame until the current is within the zero window, or until the step

size reaches 8 minimum steps, or 0.977 V. In this event, the track routine continues to change the voltage in steps of 0.977 V without further increases in the step size. If the current is driven within the zero window by an FS voltage step, the track routine resets to the initial operating point in which no action is taken so long as the BMSP current remains within limits. If an FS voltage step causes the current to reverse polarity, the track routine begins decreasing the step size by halving and reverses the FS voltage step direction. This process amounts to a binary search of the minimum step closest to the zero-current point. When the current is, once again, within the zero window, or if the voltage step reduces to one minimum step, the track routine resets and no further action is taken so long as the current remains within limits.

If the Satellite exceeds + 500 V, the FS bias voltage will remain constant at its limit of − 500 V. Once the system returns to a state in which the zero-current point is reachable within the dynamic range of the FS, a current reversal would be seen and the track routine would continue to operate as described above.

2·4. *Experiment control and programmability.* – The TSS satellite provides an uplink command rate of 2 kb/s and an average power of 50 W for the science instruments. Much of the ROPE electronics and control algorithm design was driven by these limitations. For example, to minimize the amount of uplink traffic required to change the ROPE configuration, a catalog of «Macro commands» was stored in an onboard ROM which could be accessed by a single 16-bit word. The Macro command then served as a pointer to an array of stored commands that reconfigured the various components of ROPE. Sixty-nine Macro commands were pre-programmed for the TSS-1 mission. Sixty-two of these commands could reconfigure the DIFP, SPES, and FS subsystems while seven of these commands could reconfigure only the two SPES sensor banks. ROPE commanding is not limited to Macro commands and any of the instrument commands can be transmitted to allow a vast range of instrument configurations — but at the expense of higher command traffic.

The utility of the Macro commands is their usage for the basic 12-min or 24-min Standard Operating Cycles planned for tether current flow operations (see tables II-V of Dobrowolny and Stone [1]). Each cycle consisted of six steps of 2- or 4-min duration each. Since the step duration is not an integral multiple of the ROPE command execution frequency (65.536 s), a special technique had to be used to optimize the ROPE sensor ranges for each step. Basically a sequence of 15 or 16 commands is sent to the CEP command buffer prior to the start of a 12-min cycle, 26 or 27 commands for a 24-min cycle. The CEP executes one command every fourth major frame (65.536 s), sequentially moving through the command buffer. Many commands are necessarily repeated and essentially serve as place holders in order for the optimum sensor range to be maintained for the required duration.

As mentioned in Dobrowolny and Stone [1], the maximum tether length achieved during the TSS-1 mission was 268 meters, corresponding to a maximum e.m.f. of 60 V between the satellite and the Orbiter. Because of the deployment anomaly, ROPE control functions were executed at satellite potentials of only a few volts. The planned TSS-1 timeline was halted and only a few Standard Operating Cycles were executed.

3. – Performance.

To illustrate the characteristic response of the ROPE components, data from the TSS-1 mission will be shown. Operation of the interactive control of the BMSP potential is shown in fig. 5. The top panel shows the current collected by the BMSP surface with positive values indicating electron collection. The bottom panel shows the magnitude of the BMSP potential as determined by the FS output. These data were obtained when the satellite was deployed 268 meters. A Macro command activated the SPES subsystem and initiated the FS «seek and track» routine. It was fortunate that this command was executed during step 2 of a DEP 101 cycle so that a non-zero value of the BMSP current existed before the start of the seek phase. The beginning of the seek phase is clearly seen by the sharp decrease in the BMSP current in response to the change in voltage bias. The current goes to negative values thereby stopping the seek phase and starting the slower track phase. Since the current is negative and outside the neighborhood around zero, the potential must be reduced in order to drive the net current toward zero. This part of the routine is clearly observed in the middle portion of the plot. However, once the potential is near zero volts the BMSP current is also near zero. Note that before seek was initiated, the potential was zero and the current was about 36 μA. Clearly a discrepancy exists. The oscillations that appear at the end of the time period shown confirm this fact. The oscillations are not a plasma effect and are due to an internal control loop oscillation within the FS. No problem exists for FS bias voltages less than − 10 V. For FS bias voltages greater than − 10 V, the commandibility rate is greater than 16 ms. Hence, a beating effect will occur between the commanded

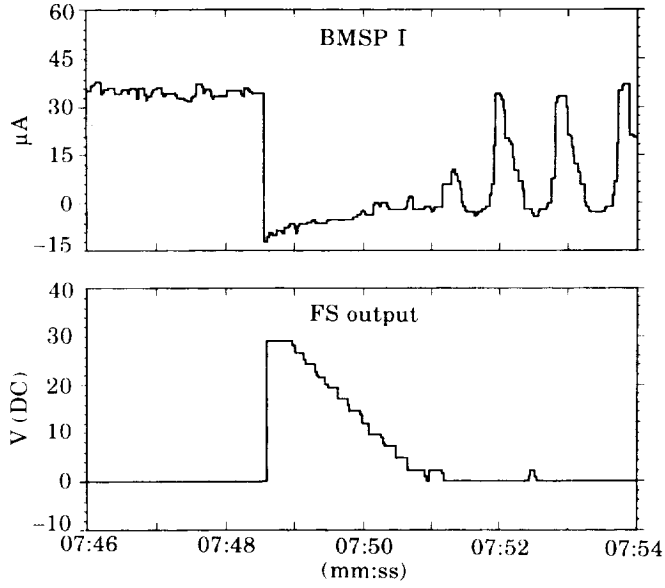

Fig. 5. – Execution of the BMSP «seek and track» operation obtained during the TSS 1 mission while the satellite was deployed. These data were acquired at night during the execution of step 2 of a DEP 101 operational sequence (1992/218/02:07:45.991).

voltage and the actual output voltage. This problem will be corrected for any reflights of TSS.

An instrument cycle for the DIFP peak detect mode is shown in fig. 6. These data were obtained when the satellite was deployed 268 meters from the Orbiter during a night time pass. The FPEG was firing during step 1 of a DEP 101 operating cycle. The SETS CMS switch was open so that the satellite was floating. Figure 6*a*) displays the intrument response for a deflection voltage sweep. Two distinct ion streams are observed with the possiblity of a third stream existing at the higher positive deflection voltages. Note that the widths of the two peaks are markedly different. This may result from a larger angular spread and/or higher energy for the stream with the broader peak. The RPA analysis of each stream shown in fig. 6*b*) and 6*c*) shows the broad-peaked stream to have a higher energy. The energy for the stream labeled 2 is approximately correct for ionospheric O^+ ions which have a ram energy of about 5 eV. Assuming stream 2 to be O^+, the fit of the retard sweep data to the standard, planar RPA equation indicates that the BMSP potential was + 0.8 V relative to the plasma. When this potential is used in the fit for stream 1, the drift energy of this stream is found to be 15 eV. Figure 6*d*) gives the plasma properties for each stream. Both streams are incident at the DIFP in the negative direction (see fig. 2*b*)). The angle resolved by the DIFP is the projection of the ion velocity in the satellite (X_B, Y_B)-plane (see fig. 2*b*)). The out-of-plane angle, *i.e.* the component of ion velocity in the (Z_B, X_B)-plane, is not

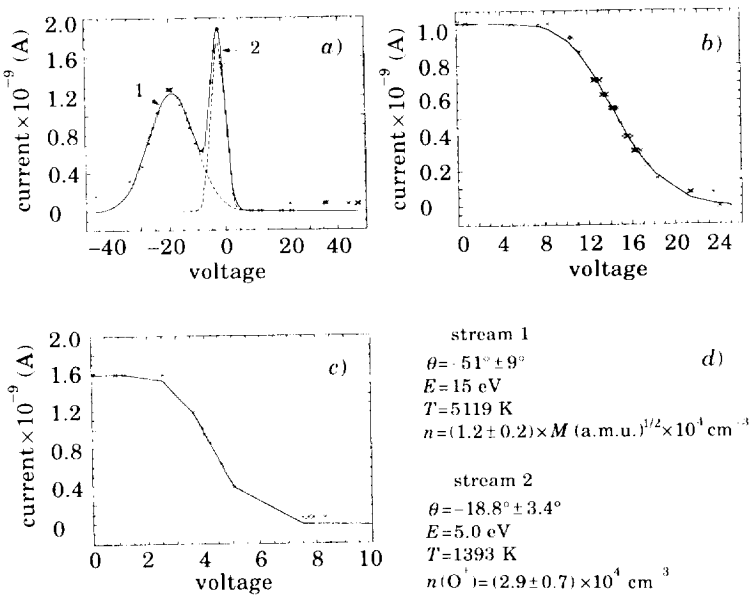

Fig. 6. — DIFP measurements in the peak detect mode obtained during the TSS-1 mission while the satellite was deployed at GMT 218/02 : 12 : 18. Data were acquired at night during the execution of the first step of a DEP 101 operational sequence. In this step FPEG was firing with the SETS CMS open — the satellite was isolated from the Orbiter. *a*) Deflection curve: « × 1» = — 19.0 V, « × 2» = — 2.5 V, *b*) retard curve 1, energy = 15.0 eV, body potential = 0.8 V, temperature = 5119 K; *c*) retard curve 2, energy = 5.0 eV, body potential = 0.8 eV, temperature = 1393 K.

measured. It is speculated that stream 1 is composed of pick-up ions from shuttle or satellite outgassing.

The SPES instrument response is displayed in fig. 7. Ion data from SPES 1 acquired at the same time as the DIFP data discussed above are shown in fig. 7*a*). Recall from fig. 2 that both the DIFP and SPES 1 point at the satellite. The count *vs.* energy spectrum has been converted to a distribution function for hydrogen ions. The spectrum is fitted by a Maxwellian distribution with the plasma properties noted at the side. To correct for any other mass, simply multiply the density by $M(\text{a.m.u.})^{1/2}$ and the velocity by $M(\text{a.m.u.})^{-1/2}$. Note that only one drifting population is observed with an energy of approximately 42 eV. SPES 1 does not detect the two drifting populations observed by the DIFP — apparently because they lie outside of the SPES 1 field of view. This third ion population, observed by SPES-1, is too low in density to be observed by the DIFP. However as noted above, the DIFP data do contain a hint of this stream. The DIFP and SPES-1

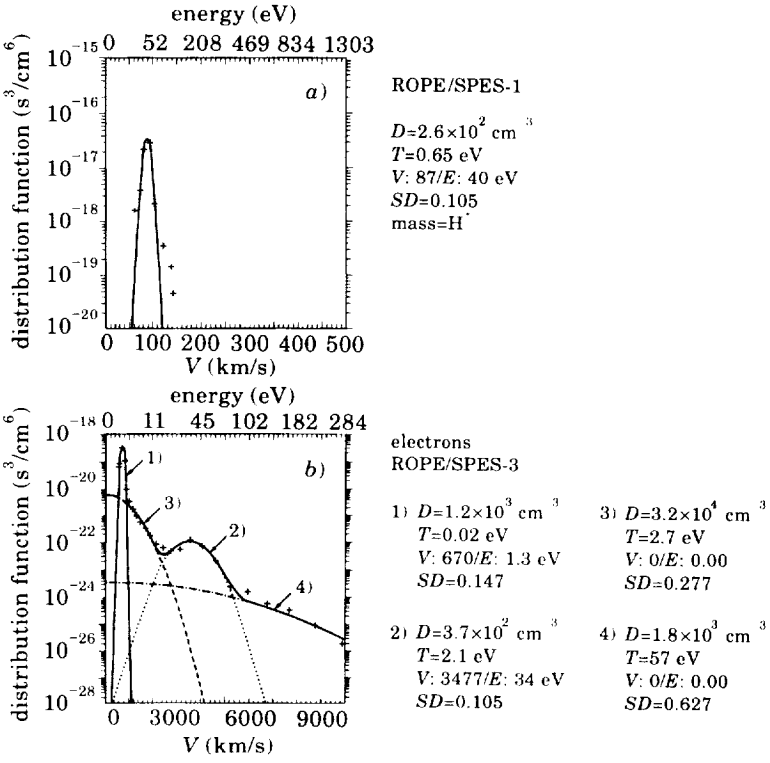

Fig. 7. – SPES instrument sweep obtained during the TSS-1 mission while the satellite was deployed. *a*) Ion data from SPES-1 at the same time as the DIFP data shown in fig. 6 (1992/218/02:12:18.823 to 02:12:20.807). *b*) Electron data from SPES-3 acquired at night during the execution of step 2 of a DEP 101 operational sequence. In this step FPEG was fired with the SETS CMS and shunt closed (1992/218/17:19:57.196 to 17:19:59.180).

measurements complement each other in that the DIFP covers a large angular range while SPES-1 has a much greater sensitivity. For the data shown in fig. 6 and 7*a*) two pick-up ion populations exist in addition to the rammed ionosphere.

Electron observations by SPES-3 are displayed in fig. 7*b*). Note that these data were obtained several hours later than the ion data discussed above. The satellite was 236 meters from the Orbiter during the night time phase of an orbit. The FPEG was firing as part of step 2 of a DEP 101 operational cycle with the SETS CMS and shunt closed. An approximate current of 17 mA was collected by the satellite and conducted through the tether. The electron spectra is described very well by four Maxwellian populations. The electrons drifting at 1.3 eV indicate that the satellite is charged to + 1.3 V. The higher energy population drifting at 34 eV is speculated to have been involved in the ionospheric current closure process between the satellite and the Orbiter. The other two populations could be evidence of a photoelectron environment near the satellite.

* * *

The authors would like to thank the engineers at Southwest Research Institute (A. Blevins, P. Jensen, R. Frahm, R. Bowman, J. Alexander) and at the Marshall Space Flight Center (D. Smith, B. Lewter, B. Chisholm) for their dedication and persistence in seeing this project completed. Special thanks go to G. Johnston of the MSFC/TSS Project Office who served as experiment manager. In addition, thanks are extended to the engineers of Alenia Spazio who supported this experiment during satellite integration and testing and during the TSS-1 mission. Co-Investigators who will be providing theoretical and data analysis support are: J. Burch (Southwest Research Institute), D. S. Intriligator (Carmel Research Center), U. Samir (Univ. of Michigan), R. W. Schunk (Utah State Univ.), N. Singh and S. T. Wu (both at Univ. of Alabama in Huntsville). KHW acknowledges support from NASA under contract NAS8-37107. JDW, JB, and CG acknowledge support from NASA under contract NAS8-36840.

REFERENCES

[1] M. DOBROWOLNY and N. H. STONE: this issue, p. 1.
[2] N. H. STONE: *Rev. Sci. Instrum.*, **48**, 1458 (1977).
[3] N. H. STONE, B. J. LEWTER, W. L. CHISHOLM and K. H. WRIGHT jr.: *Rev. Sci. Instrum*, **56**, 897 (1985).
[4] W. J. HEIKKILA, J. B. SMITH, T. TARSTRUP and J. D. WINNINGHAM: *Rev. Sci. Instrum.*, **41**, 1393 (1970).
[5] J. D. WINNINGHAM, J. L. BURCH, N. EAKER, V. A. BLEVINS and R. A. HOFFMAN: *Space Sci. Instrum.*, **5**, 465 (1981).
[6] J. D. WINNINGHAM *et al.*: *J. Goephys. Res.*, **98**, 649 (1993).
[7] F. BORDONI: *Nucl. Instrum. Methods*, **97**, 405 (1971).